ACS NANO
Cite This: ACS Nano 2018, 12, 4378−4386
www.acsnano.org

ARTICLE

Turning On/Off the Anti-Tumor Effect of the Au Cluster via Atomically Controlling Its Molecular Size

Jiao Zhai,[‡,§] Yanwei Jia,[‡] Lina Zhao,[§] Qing Yuan,[†,§] Fuping Gao,[§] Xiangchun Zhang,[§] Pengju Cai,[§] Liang Gao,[†] Juanjuan Guo,[§] Shuhong Yi,[⊥] Zhifang Chai,[§] Yuliang Zhao,[§] and Xueyun Gao*[,†,§]

[†]Department of Chemistry and Chemical Engineering, Beijing University of Technology, Beijing 100124, China
[‡]State Key Laboratory of Analog and Mixed Signal VLSI, University of Macau, Macao, SAR, China
[§]CAS Key Laboratory for Biological Effects of Nanomaterials and Nanosafety, Institute of High Energy Physics, Chinese Academy of Sciences, Beijing 100049, China
[⊥]Liver Transplantation Center, the Third Affiliated Hospital, Sun Yat-sen University, Guangzhou 510000, China

Supporting Information

ABSTRACT: We reported two Au clusters with precisely controlled molecular size ($Au_5Peptide_3$ and $Au_{22}Peptide_{10}$) showing different antitumor effects. *In vitro*, both $Au_5Peptide_3$ and $Au_{22}Peptide_{10}$ were well taken up by human nasopharyngeal cancer cells (CNE1 cells). However, only $Au_5Peptide_3$ significantly induced CNE1 cell apoptosis. Further studies showed that CNE1 cells took up $Au_5Peptide_3$ (1.98×10^{-15} mol/cell), and 9% of them entered mitochondria (0.186×10^{-15} mol/cell). As a comparison, the uptake of $Au_{22}Peptide_{10}$ was only half the amount of $Au_5Peptide_3$ (1.11×10^{-15} mol/cell), and only 1% of them entered mitochondria (0.016×10^{-15} mol/cell). That gave 11.6-fold more $Au_5Peptide_3$ in mitochondria of CNE1 cells than $Au_{22}Peptide_{10}$. Further cell studies revealed that the antitumor effect may be due to the enrichment of $Au_5Peptide_3$ in mitochondria. $Au_5Peptide_3$ slightly decreased the Mcl-1 (antiapoptotic protein of mitochondria) and significantly increased the Puma (pro-apoptotic protein of mitochondria) expression level in CNE1 cells, which resulted in mitochondrial transmembrane potential change and triggered the caspase 9−caspase 3−PARP pathway to induce CNE1 cell apoptosis. *In vivo*, CNE1 tumor growth was significantly suppressed by $Au_5Peptide_3$ in the xenograft model after 3 weeks of intraperitoneal injection. The TUNEL and immuno-histochemical studies of tumor tissue verified that CNE1 cell apoptosis was mainly via the Puma and Mcl-1 apoptosis pathway in the xenograft model, which matched the aforementioned CNE1 cell studies *in vitro*. The discovery of Au_5 but not Au_{22} suppressing tumor growth via the mitochondria target was a breakthrough in the nanomedical field, as this provided a robust approach to turn on/off the nanoparticles' medical properties via atomically controlling their sizes.

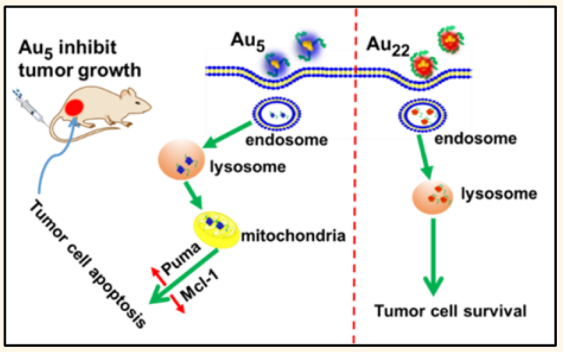

KEYWORDS: *peptide−Au cluster, antitumor effect, mitochondria, Puma, Mcl-1, cell apoptosis*

In the past two decades, size-controlled nanoparticles have been widely pursued because size plays a key role in tuning their basic physical, chemical, and biological properties.[1] To date, it is still difficult to precisely synthesize nanoparticles with exact molecular formula and size.[2] This leads to variable, rather than consistent, properties even for the same batch of nanoparticles. because such nanoparticles are not identical with each other and chemical molecules are.[3] Therefore, controlling nanoparticles with precise molecular formula and size has been a dream for researchers for a long time. Fortunately, this issue has been resolved in the case of metal clusters.[4] Metal clusters possess several to several hundreds of atoms with precise molecular formula and size,[5] showing molecule-like properties, such as ferromagnetism,[6] photoluminescence,[7] and quantum behavior.[8] Based on these properties, Au clusters have been widely applied in biosensing and bioimaging,[9] tumor diagnosis, and therapy.[10,11] Recently, Jie Zheng et al. reported that Au_{11} and Au_{25} have very different metabolism behaviors *in vivo* because cluster size plays the key role in the tissue passive/filtrate process.[12] We hypothesize that via atomically tuning the size of Au clusters, they may have an on/off state in suppressing

Received: January 4, 2018
Accepted: April 18, 2018
Published: April 18, 2018

DOI: 10.1021/acsnano.8b00027
ACS Nano 2018, 12, 4378−4386

tumor growth *in vivo/vitro*. If this hypothesis was proven, a very interesting tumor treatment approach would be discovered in the nanomedical field.

RESULTS AND DISCUSSION

We have reported that peptides could reduce Au ions to produce Au clusters with precise molecular formula and size.[13] In this work, we designed the H_2N-YHWYGYTPQNVI-KKKK-YCC-COOH peptide with two functional domains. YHWY-GYTPQNVI was the specific target sequence for the epidermal growth factor receptor (EGFR),[14] while YCC was applied to capture the Au cluster via the Au−S bond. KKKK was incorporated to increase the solubility of the peptide. This peptide was used to synthesize Au clusters with different molecular sizes. After being synthesized and purified, the Au clusters were analyzed by mass spectra and fluorescence spectra. Although ESI-MS is a softer technique to characterize the Au nanoclusters,[15,16] it is difficult to obtain good spectra for large molecular weighted thiolate ligands, such as protein and long chain polypeptides. Therefore, matrix-assisted laser desorption/ionization time-of-flight mass spectrometry (MALDI-TOF-MS) was utilized to study the mass and to determine the molecular formula of each Au cluster.[17,18] As depicted in Figure 1a, the spectrum of the one peptide-coated Au cluster was composed of 5 Au atoms, 6 sulfur atoms, and 1 or 2 sodium atoms. We could not get the intact composition of this cluster (Figure S1), because the C−S bond of the peptide was easily broken during the laser desorption process.[18] As one peptide was with two S atoms, we could assign this Au cluster as $Au_5Peptide_3$. In Figure 1b, the mass spectrum of another peptide-coated Au cluster was very clear, and its molecular formula was assigned as $Au_{22}Peptide_{10}$. The fluorescence spectra of the $Au_5Peptide_3$ and $Au_{22}Peptide_{10}$ showed maximum emission at 408 and 655 nm, respectively (Figure 1c (blue line),d (red line)), with strong blue and red fluorescence under UV excitation (insets of Figure 1c,d), providing a convenient way to monitor the cellular distribution of each Au cluster in the following experiments. The surface charges for $Au_5Peptide_3$ and $Au_{22}Peptide_{10}$ were −34.53 ± 0.72 and −43.73 ± 1.62 mv, respectively, indicating the stability of the two sized clusters.

The human nasopharyngeal carcinoma cell line CNE1[19] was used to study the cell toxicity and apoptosis induced by $Au_5Peptide_3$, $Au_{22}Peptide_{10}$, or peptide alone as a control study. The cytotoxicity was determined by the colorimetric cck-8 assay. The results showed that $Au_5Peptide_3$ induced more than 50% cell death when the CNE1 cells were exposed to Au clusters for 24 h (Au 80 μM, blue bar in Figure 1e). Most CNE1 cells were dead when they were treated with $Au_5Peptide_3$ for 48 h (Figure 1g). However, $Au_{22}Peptide_{10}$ (Au 80 μM, red bar in Figure 1e) and free peptide (peptide 100 μM, green bar in Figure 1f) showed almost no cell toxicity to the CNE1 cells after incubation for 24 h, even up to 48 h (Figure 1g). In addition, for the EGFR negative MCF-7 cell line and normal human 16HBE cell line, none of $Au_5Peptide_3$, $Au_{22}Peptide_{10}$, or free peptide showed cell toxicity when the cells were incubated for up to 48 h (Au 80 μM, peptide 100 μM, Figures S2 and S3). These results suggested that $Au_{22}Peptide_{10}$ or peptide had no cell toxicity for the EGFR positive CNE1 cell, EGFR negative MCF-7 cell, and normal EGFR 16HBE cell. Only the smaller sized $Au_5Peptide_3$ had a cytotoxic effect in the EGFR positive CNE1 cell as a function of the cell incubation time and Au concentration (Figure 1e,g).

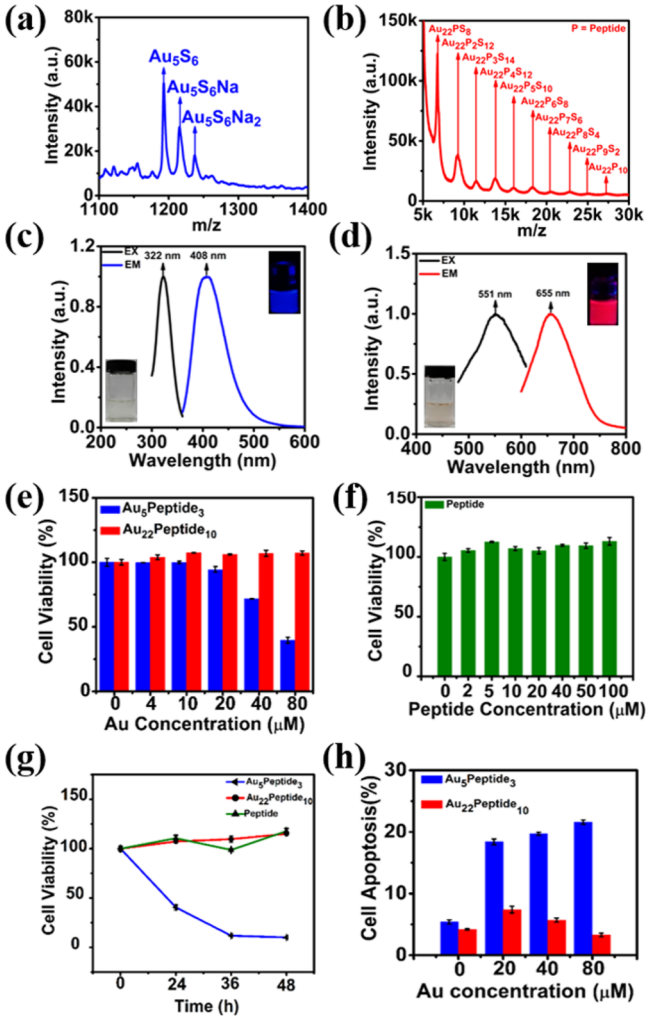

Figure 1. Characterization of peptide−Au clusters (a−d) and cell toxicity/apoptosis induced by the Au clusters (e−h). MALDI-TOF-MS of (a) $Au_5Peptide_3$ and (b) $Au_{22}Peptide_{10}$. S and P in (a) and (b) represent sulfur and peptide, respectively. (c,d) The excitation and emission spectra of $Au_5Peptide_3$ and $Au_{22}Peptide_{10}$. Insets in (c) and (d) are Au cluster photographs taken without (lower left) and with (upper right) 365 nm ultraviolet light irradiation. (e) The cck-8 results of CNE1 cells treated with a series of concentrations of Au clusters and (f) the corresponding free peptide for 24 h. (g) The CNE1 cell viability depending on the Au cluster incubation time at a fixed Au concentration of 80 μM. (h) The CNE1 cell apoptosis induced by $Au_5Peptide_3$ and $Au_{22}Peptide_{10}$, respectively, when treated with a series of Au doses for 24 h.

We further chose BSA, with no affinity to EGFR, as the surface coating ligand, to synthesize smaller sized Au nanoclusters and explore its cytotoxicity to the EGFR positive CNE1 cells. The result in Figure S4 suggested that smaller sized BSA-Au clusters had no obvious cytotoxicity in the same tested range of the Au concentration. All of these results suggested that the peptide could help $Au_5Peptide_3$ to enter the EGFR positive cells and induce cell death. We further performed Annexin V-FITC/PI staining analysis to assess the CNE1 cell apoptosis when they were treated by the $Au_5Peptide_3$ or $Au_{22}Peptide_{10}$. Flow cytometry analysis results (Figures 1h and S6) showed that CNE1 cell apoptosis was about 5.3, 18.4, 19.7, and 21.6% when cells were exposed to $Au_5Peptide_3$ at Au concentration of 0, 20, 40, and 80 μM for 24 h, respectively. However, $Au_{22}Peptide_{10}$ caused 3.3% CNE1 cell apoptosis, and this value was

DOI: 10.1021/acsnano.8b00027
ACS Nano 2018, 12, 4378−4386

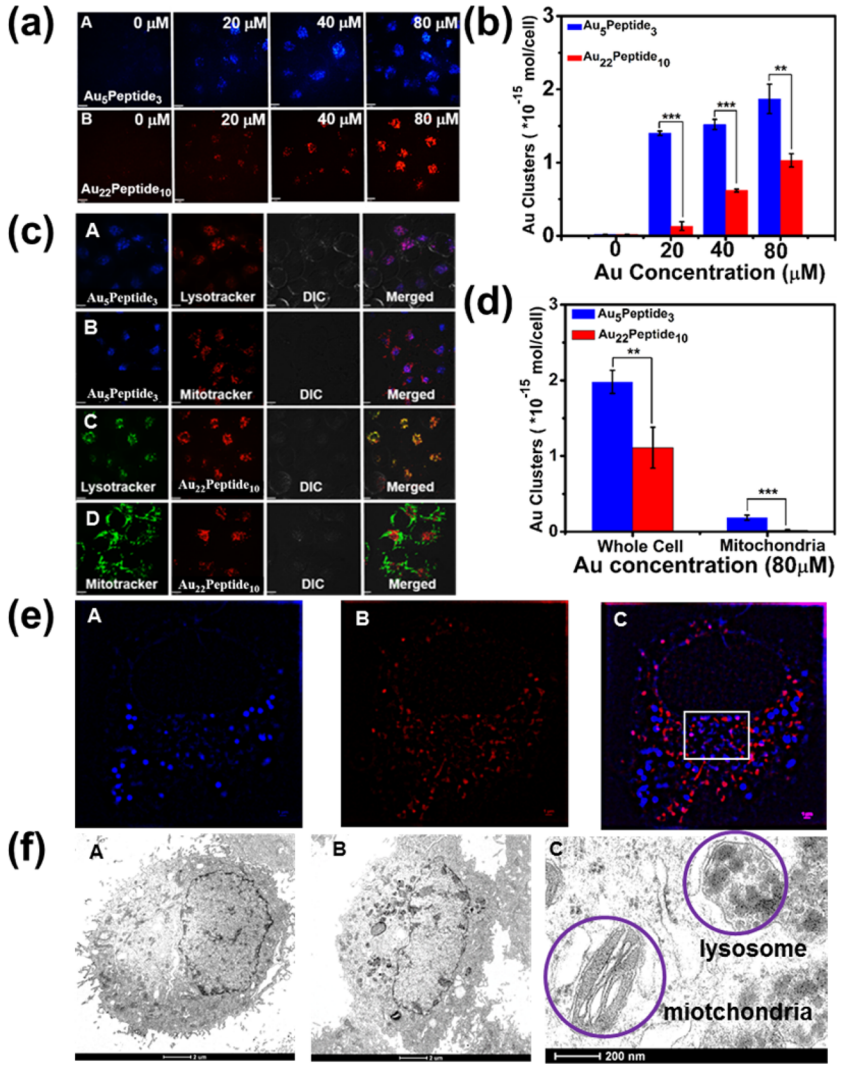

Figure 2. Cell uptake (a,b) and subcellular location (c,d) of $Au_5Peptide_3$ and $Au_{22}Peptide_{10}$ in CNE1 cells. (a-A,B) Confocal microscopy images of CNE1 cells exposed to $Au_5Peptide_3$ and $Au_{22}Peptide_{10}$ with several Au concentrations for 24 h. (b) The ICP-MS result of the cell uptake of the Au cluster corresponded to (a-A) and (a-B). (c) Confocal microscopy images of CNE1 cells exposed to $Au_5Peptide_3$ and $Au_{22}Peptide_{10}$ for 24 h at 80 μM Au and then 50 nM lysotracker (c-A,C) or 50 nM Mitotracker (c-B,D) staining cells for 20 min, respectively. (d) ICP-MS result of $Au_5Peptide_3$ and $Au_{22}Peptide_{10}$ in the whole cell and the cell extracted mitochondria (Au 80 μM, incubation time was 24 h). (e) The reconstructed imaging of the structured-illumination high resolution images (e-A) for CNE1 cells exposed to $Au_5Peptide_3$ (80 μM Au, 24 h), followed by mitotracker staining (e-B), and the merged image (e-C). (f) TEM images of CNE1 cells exposed to $Au_5Peptide_3$ at 80 μM Au for 24 h (f-B), control cells (f-A), and the higher magnification images of f-B (2f-C).

comparable with the no Au cluster-treated control cells (4.2% cell apoptosis, Figures 1h and S7). In other words, $Au_{22}Peptide_{10}$ had no cell apoptosis effect on CNE1 cells. This study revealed that only $Au_5Peptide_3$ could strongly induce CNE1 cells apoptosis *in vitro*.

For CNE1 cell toxicity and apoptosis, what caused the big difference between $Au_5Peptide_3$ and $Au_{22}Peptide_{10}$? To answer this question, the cell uptake and subcellular distribution of $Au_5Peptide_3$ and $Au_{22}Peptide_{10}$ were studied by confocal microscopy and structured-illumination microscopy (SIM) and inductively coupled plasma mass spectrometry (ICP-MS) and TEM, respectively. Confocal microscopy images in Figure 2a show CNE1 cells could take up both $Au_5Peptide_3$ (blue fluorescence) and $Au_{22}Peptide_{10}$ (red fluorescence). The ICP-MS results in Figure 2b showed that the cell uptake of $Au_5Peptide_3$ and $Au_{22}Peptide_{10}$ had positive correlations with Au concentrations in cell culture media. The CNE1 cells took up $Au_5Peptide_3$ $\sim 1.98 \times 10^{-15}$ mol/cell and $Au_{22}Peptide_{10}$ $\sim 1.11 \times 10^{-15}$ mol/cell at an Au dose of 80 μM in cell culture media. This result showed that $Au_5Peptide_3$ entered more easily into the cell than $Au_{22}Peptide_{10}$. As the EGFR expression level was high in the CNE1 cell membrane,[19,20] the strong affinity between EGFR and Au clusters may assist Au clusters entering cells. Besides, cell viability studies with EGFR-blocked cells treated with $Au_5Peptide_3$ supported the hypothesis that EGFR affinity played an important role in Au cluster internalization by tumor cells (Figure S5).

To further investigate the subcellular location of Au clusters, lysotracker and mitotracker were employed. The confocal microscopy images in Figure 2c suggested that $Au_5Peptide_3$ was mainly located in lysosomes (Figure 2c-A), and some of them entered mitochondria (Figure 2c-B). Whereas, $Au_{22}Peptide_{10}$ was mostly located in lysosomes (Figure 2c-C), and it was hardly to be found in mitochondria (Figure 2c-D). According to the ICP-MS experiments, CNE1 cells took up $\sim 1.98 \times 10^{-15}$ $Au_5Peptide_3$ mol/cell and $\sim 1.11 \times 10^{-15}$ $Au_{22}Peptide_{10}$ mol/

DOI: 10.1021/acsnano.8b00027
ACS Nano 2018, 12, 4378−4386

cell, as shown in Figure 2d. However, for mitochondria localization there was ~0.186 × 10^{-15} $Au_5Peptide_3$ mol/cell but only ~0.016 × 10^{-15} $Au_{22}Peptide_{10}$ mol/cell. That means about 9% of $Au_5Peptide_3$ located in mitochondria, 10 times more than that of $Au_{22}Peptide_{10}$ (about 1%). This indicated that only $Au_5Peptide_3$ but not $Au_{22}Peptide_{10}$ could enter the mitochondria, although the detailed mechanism is still not clear now. To further confirm $Au_5Peptide_3$ could target and concentrate in mitochondria of CNE1 cells, structured-illumination microscopy was used to observe the $Au_5Peptide_3$ location in CNE1 cells (80 μM Au and 24 h cell incubation, following mitotracker staining). The reconstruction image in Figure 2e shows that the Au_5 clusters (blue, A) co-localized with mitotracker stained mitochondria (red, B) and generated a purple color (C). The TEM images of $Au_5Peptide_3$-treated CNE1 cells further confirmed that Au_5 clusters are located in the lysosome and mitochondria due to the high density contrast of Au (Figure 2f-B) when compared with the no Au cluster-treated control cells (Figure 2f-A). The higher magnification images of $Au_5Peptide_3$-treated cells revealed that $Au_5Peptide_3$ was clearly confined in the lysosome and mitochondria given the high contrast of the Au cluster therein (Figure 2f-C). All of this evidence implied that the cytotoxic and cell apoptosis should be attributed to the mitochondria localization of the Au_5 cluster but not the Au_{22} cluster.

The aforementioned results implied that $Au_5Peptide_3$ may meditate cell apoptosis via a mitochondria-dependent pathway. As well-known, the Bcl-2 family proteins play important roles in the mitochondrial apoptotic pathway,[20,21] as they can perturb the mitochondrial membrane integrity[21,22] and induce cytochrome c release from mitochondria to cytoplasm.[23] It is also known that the up-regulation of pro-apoptotic protein (bid, bim, and Puma) and/or the down regulation of anti-apoptotic (bcl-2, bcl-xl, and Mcl-1) could trigger cell apoptosis. Here we first checked if $Au_5Peptide_3$ could change the bcl-2 family protein expression level in CNE1 cells. The Western blot results of $Au_5Peptide_3$-treated CNE1 cells in Figure 3a revealed that the expression level of pro-apoptotic Puma significantly increased in an Au dose-dependent manner in the range of 0–80 μM, and the anti-apoptotic Mcl-1 level was obviously down-regulated at an Au dose of 80 μM. Upregulation of Puma expression[24,25] and down-regulation of Mcl-1 expression would initiate cell apoptosis.[26,27] Note that the Au_5 cluster mainly increased the Puma expression level and moderately decreased the Mcl-1 level (Figure 3a). Once the Puma and Mcl-1 initiated the depolarization of the mitochondrial membrane, they would further induce cytochrome c release from the mitochondria to the cytoplasm and activate serial pro-apoptotic molecules therein. In this study, the JC-1 fluorescent probe was used to detect the changes of the mitochondrial membrane potential (MMP). JC-1 forms aggregates and emits red fluorescence at high MMP. If MMP was losing, some JC-1 would exist as monomers with green fluorescence emission. Figure 3b depicted that JC-1 exhibited bright red and weak green fluorescence in the control CNE1 cells. When the cells were treated with carbonyl cyanide *m*-chlorophenyl hydrazine (CCCP), MMP decreased significantly and resulted in a very strong green and weak red fluorescence emission. When CNE1 cells were treated with $Au_5Peptide_3$ (Au 80 μM and incubation 24 h), they exhibited bright green fluorescence and faint red fluorescence. This revealed that $Au_5Peptide_3$ can decrease the MMP via strong up-regulation of Puma and mild down-regulation of Mcl-1. We further examined the level of

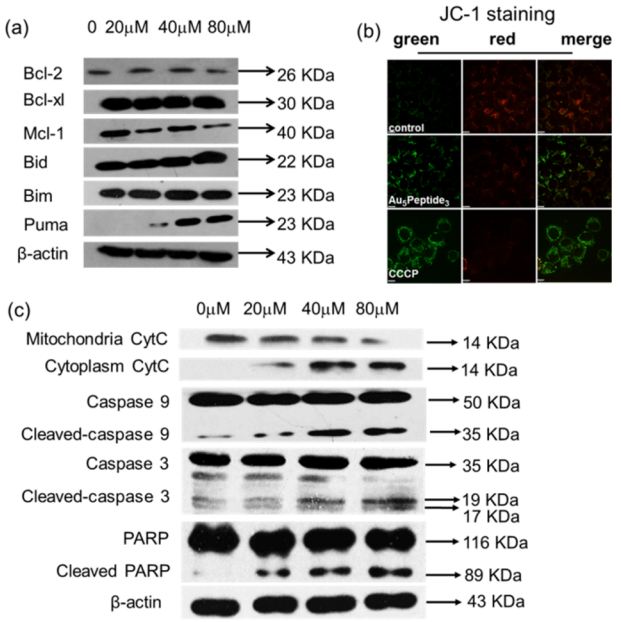

Figure 3. (a) Western blot of bcl-2 family protein expression levels in cells treated with a serial dose of $Au_5Peptide_3$ for 24 h. (b) The study of the mitochondrial membrane potentials of CNE1 cells by confocal microscopy after being incubated with $Au_5Peptide_3$ (Au 80 μM, 24 h) and CCCP (1.0 μg/mL and incubation 24 h), respectively, and further staining by JC-1 for confocal observations. (c) Western blot of CytC, caspase-9, caspase-3, PARP, and their cleaved form after $Au_5Peptide_3$ treatment (Au concentration was 0, 20, 40, and 80 μM, and incubation time was 24 h). β-actin was used as the internal control.

cytochrome c in the cytoplasm and mitochondria, respectively. Western blot results in Figure 3c show that the level of cytochrome c gradually decreased in the mitochondrial extraction, whereas it increased in the cytoplasmic extraction. Once cytochrome c was released to cytoplasm, it would combine with the apoptotic protease-activating factor-1 and procaspase-9 to form an apoptosome. Then, caspase-9 would be activated to become the initiator caspase and activate the effector caspase-3.[28] Subsequently, the effector caspase-3 would cleave cellular substrates, such as PARP, to trigger cell apoptosis.[29] To investigate whether caspase-9, caspase-3, and PARP were activated by $Au_5Peptide_3$, Western blot of the intact and cleaved caspase-9, caspase-3, and PARP were performed. The results in Figure 3c revealed that intact caspase-9, caspase-3, and PARP were cleaved to active 35, 17/19, and 89 kDa fragments when CNE1 cells were treated with $Au_5Peptide_3$. When the Au concentration increased from 0 to 80 μM in cell culture media (incubation 24 h), the level of cleaved caspase-9, caspase-3, and PARP significantly increased in an Au dose-dependent manner.

The *in vivo* antitumor effects of $Au_5Peptide_3$ or free peptide were studied by intraperitoneal injection of serial dosages of $Au_5Peptide_3$ or free peptide in the CNE1 tumor xenograft model, respectively. Note that the CNE1 tumor grows quickly in the xenograft model. Therefore, the Au clusters could only treat the tumor for up to 21 days in the CNE1 xenograft model. Figure 4a,b shows that $Au_5Peptide_3$ significantly inhibited the tumor growth ($P < 0.01$) at the Au dosage of 15 mg/kg once every 2 days when compared with the saline- or free peptide-treated CNE1 tumor for 21 days. For 10 days of treatment, both the low and high dosages of $Au_5Peptide_3$ (10 and 15 mg/

DOI: 10.1021/acsnano.8b00027
ACS Nano 2018, 12, 4378–4386

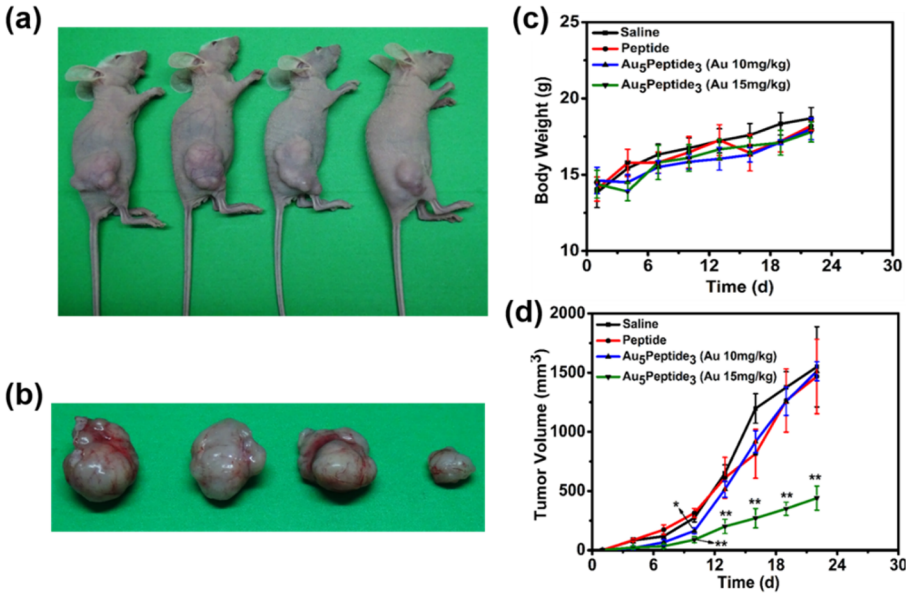

Figure 4. Photographs of (a) mice bearing CNE1 tumors and (b) corresponded tumors when the nude mice are implanted with CNE1 and further treated with Au clusters, peptide, saline for 21 days. From left to right is the saline group, peptide (110 mg/kg) group, $Au_5Peptide_3$ (Au, 10 mg/kg) group, and $Au_5Peptide_3$ (Au, 15 mg/kg) group. (c) The average nude mice body weight and (d) the average tumor volume of each group at a different time point (* or ** denotes statistical significance. *, $p < 0.05$, **, $p < 0.01$, compared with saline group).

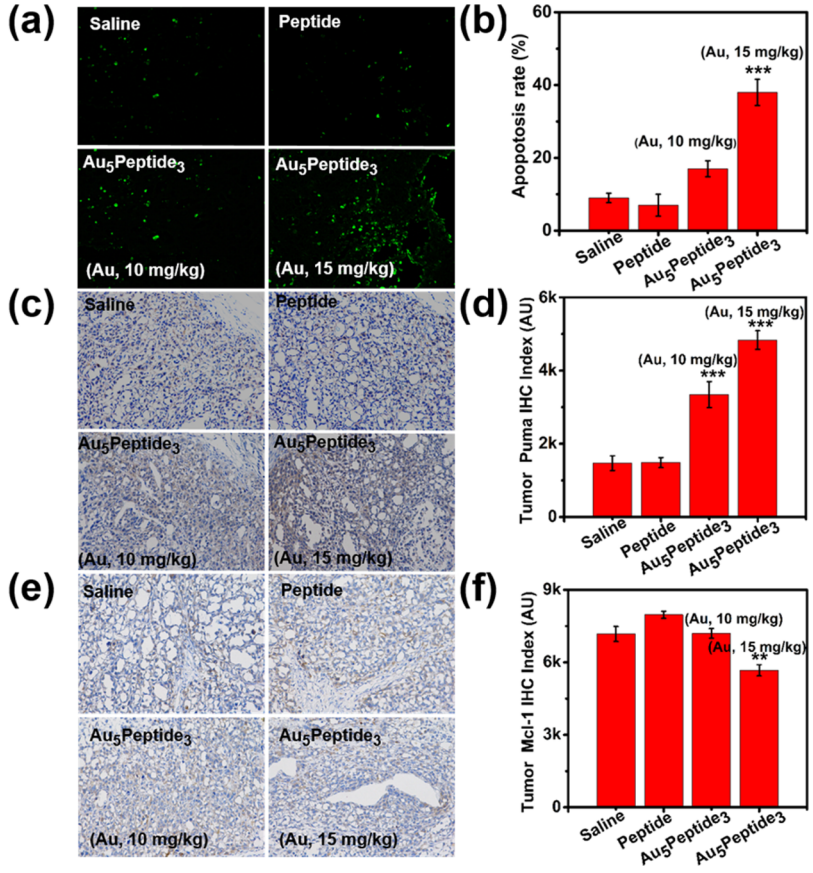

Figure 5. (a) TUNEL results of the tumor tissues of each treated mice group. Magnification ×200. (b) Quantification of apoptosis CNE1 cells corresponded to (a). Immunohistochemical detection of Puma (c) and Mcl-1 (e) in mice tumors in each nude mice group. Quantification of (d) Puma and (f) Mcl-1 expression corresponded to (c) and (e), respectively. (** or *** denotes statistical significance. **, $p < 0.01$, ***, $p < 0.001$, compared with saline-treated group.)

kg, respectively) showed apparent antitumor effect ($P < 0.05$) when compared with the saline- or free peptide-treated model. After day 10, the low dosage of $Au_5Peptide_3$ (10 mg/kg) could not suppress the tumor growth well (Figure 4d). Free peptide

DOI: 10.1021/acsnano.8b00027
ACS Nano 2018, 12, 4378−4386

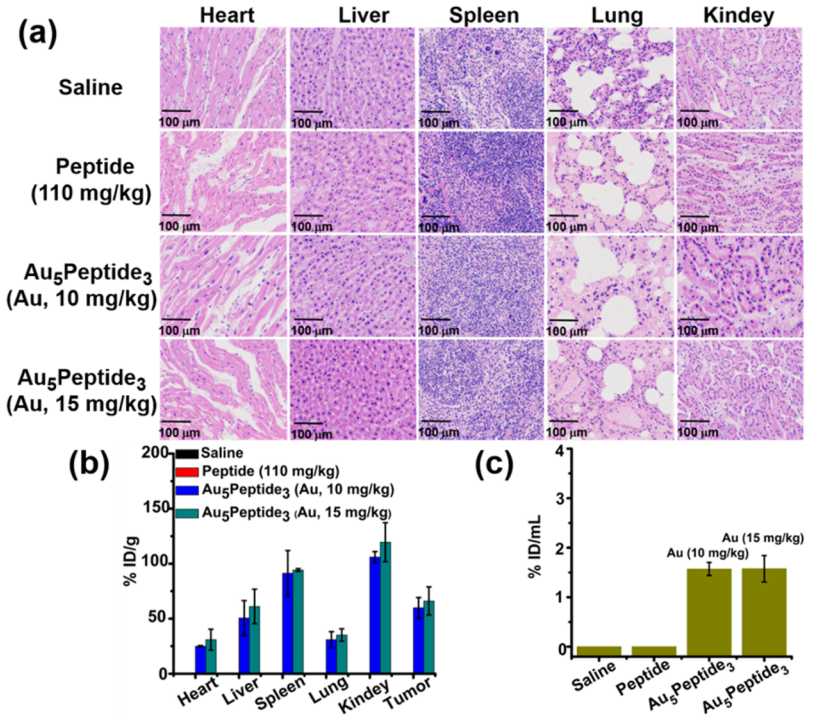

Figure 6. (a) H&E stained images of heart, liver, spleen, lung, and kidney in each nude mice group. Distribution of Au in (b) heart, liver, spleen, lung, kidney, tumor, and (c) blood in each nude mice group. The nude mice of the four groups were implanted with CNE1 and further treated by Au_5 clusters, peptide, or saline for 21 days at peptide 110 mg/kg, Au 10 mg/kg, and Au 15 mg/kg, respectively.

had no effect on tumor suppression even at a dosage of 110 mg/kg once every 2 days for 21 days. Body-weight measurement was used to evaluate the toxicity of $Au_5Peptide_3$. As depicted in Figure 4c, all of the mice in the four groups gained body weight during the study period. No body weight loss was observed in the four groups of mice. This implied that the Au cluster had no obvious toxicity for the xenograft model at the applied Au dosage.

As $Au_5Peptide_3$ up-regulated Puma and down-regulated Mcl-1 for CNE1 cells and induced cell apoptosis *in vitro* (Figure 3), we further checked if this mechanism still worked in the $Au_5Peptide_3$-treated CNE1 tumor xenograft model by immunohistochemistry studies of tumor tissues. The TUNEL staining of the tumor tissue treated with $Au_5Peptide_3$ (Figure 5a) (Au dosage of 10 and 15 mg/kg, respectively, and green fluorescence for apoptotic cells) showed that $Au_5Peptide_3$ could significantly result in tumor cell apoptosis when compared with the saline- or free peptide-treated model. The lower percentage of apoptosis in cells at 10 mg/kg of $Au_5Peptide_3$ (Figure 5b) may explain why the tumor kept growing after 10 days of administration. The Puma and Mcl-1 expression levels of the $Au_5Peptide_3$-treated CNE1 tumor were further studied. For this issue, the tumor tissues of the four groups of the xenograft model were analyzed by immunohistochemistry. Figure 5c,d showed that $Au_5Peptide_3$ (Au dosage of 10 and 15 mg/kg, respectively) significantly increased the Puma expression level in the tumor tissue compared with that of the saline- or peptide-treated mice ($P < 0.001$). The high dosage of the Au cluster (15 mg/kg) induced a significantly higher level of Puma when compared with that of the low dosage of the Au cluster (10 mg/kg). Also, $Au_5Peptide_3$ (Au dosage of 15 mg/kg) resulted in down regulation of Mcl-1 ($P < 0.01$) in the tumor tissue compared with that of the saline- or peptide-treated nude model (Figure 5e,,f). The $Au_5Peptide_3$ significantly upregulated Puma and moderately downregulated Mcl-1 and induced CNE1 apoptosis in the CNE1 tumor xenograft model, which was consistent with the results in CNE1 cell studies (Figure 3a).

Although the body weight of the Au cluster-treated mice stayed at the similar level as the saline- or peptide-treated nude mice (Figure 4c), its toxicity for different organs in mice should be further evaluated. The mice of the four groups bearing CNE1 tumors were treated by saline, peptide (110 mg/kg), $Au_5Peptide_3$ (10 mg/kg), or $Au_5Peptide_3$ (15 mg/kg) for 21 days. The tissues were stained by hematoxylin and eosin (H&E), and their pathological changes were monitored. The pathological analyses results (Figure 6a) showed that the main tissues, including the heart, liver, spleen, lung, and kidney, had no histopathological changes in all of the nude mice. Six indexes of blood biochemical and eight hematological indicators of the nude mice of the four groups were tested (Figures S8 and S9). The hematology analysis results in Figure S9 show that hemoglobin (HGB) decreased significantly ($p < 0.05$) in $Au_5Peptide_3$-treated mice (Au dosage of 15 mg/kg) compared with that of the saline group. But this HGB level was still within the normal range. No significant differences were observed in other hematology and blood biochemical assay in Au cluster-treated mice when compared with the mice treated by saline or free peptide. All of these results suggested that $Au_5Peptide_3$ had a very good biocompatibility in nude mice when they were applied to treat the CNE1 tumor in the xenograft model. Recently, Jie Zheng et al. reported that the Au_{10-11} clusters were more easily trapped in the kidney or tumor because of their very small subnanometer size. According to their studies, we speculated that our Au_5 cluster should have more retention in the kidney and tumor, as Au_5 was even smaller than Au_{10-11}. After 21 days of Au_5, peptide, and saline treatment, the biodistribution of Au in the heart, liver, spleen,

DOI: 10.1021/acsnano.8b00027
ACS Nano 2018, 12, 4378−4386

lung, tumor, kidney, and blood was studied. Figure 6b shows that most Au was accumulated in the kidney (~110% ID/g). The tumor also contained concentrated Au (~60% ID/g) in the CNE1 xenograft model. Figure 6c shows that the Au concentration in blood was very low (~1.5% ID/ml), which implied that Au clusters were mainly cleared from the mice via renal excretion, although small amount of Au was retained and accumulated in the heart, liver, lung, spleen, and tumor.

CONCLUSIONS

In summary, utilizing an artificially designed peptide, we synthesized $Au_5Peptide_3$ and $Au_{22}Peptide_{10}$. The two Au clusters have precise molecular size. Although $Au_5Peptide_3$ and $Au_{22}Peptide_{10}$ could be taken up by CNE1 cells, only $Au_5Peptide_3$ but not $Au_{22}Peptide_{10}$ had cytotoxicity/apoptosis effects on CNE1 cells in an Au dose dependent manner *in vitro*. This was because $Au_5Peptide_3$ could enter into CNE1 cell mitochondria and induce cell apoptosis via strongly upregulating Puma and moderately downregulating Mcl-1, lowering the mitochondrial transmembrane potential and triggering the caspase 9−caspase 3−PARP pathway. $Au_5Peptide_3$ also suppressed CNE1 tumor growth *in vivo* via the Puma and Mcl-1 apoptosis pathway in the xenograft model. By atomically controlling the Au cluster size, we could precisely turn on or off the antitumor effect of Au clusters. Although for clinical patients, intraperitoneal injection is rarely used in drug administration, for a potential new drug in the stage of animal experiment, intraperitoneal injection is often used as an alternative to intravenous administration, as intraperitoneal administration is good for examining a potential of this new Au cluster in the animal experiments to determine whether it is effective, its appropriate dosage form, its pharmacokinetics, and other aspects *in vivo*. This provides a robust approach to treat tumors in the earlier stages. In our studies, we analyze the different molecular configurations, including the Au cluster size and number of peptides, the result revealed that the clusters with slightly different sizes result in different suborganelles localization in the cells, which finally causes different biological or cytotoxic effects.

EXPERIMENTAL SECTION

Preparation of Peptide-Au Cluster. For $Au_5Peptide_3$ synthesis, the peptide (YHWYGYTPQNVIKKKKYCC) solution (1 mM, 515 μL) was prepared by dissolving it in ultrapure water. Then, NaOH was used to adjust the pH to 10 (the whole preparation process was carried at 42 °C). After being stirred for 5 min, $HAuCl_4$ (25 mM, 10 μL) aqueous solution was introduced with strong stirring. Subsequently, pH of the solution was adjusted to 14 by NaOH and incubated for 12 h. Finally, the product was stored away from light at 4 °C. Before being used in the subsequent experiments, the product was dialyzed (Millipore, MWCO: 3 kDa) to remove free ions and peptides. The purified sample was stored at 4 °C in the dark for later studies.

For $Au_{22}Peptide_{10}$ synthesis, 82 μL of $HAuCl_4$ (25 mM, aqueous solution) was slowly dripped into the peptide solution (1.47 mM, 1400 μL) in a 5 mL vial under vigorous stirring at room temperature (25 °C). Then, NaOH aqueous solution (0.5 M, 210 μL) was added dropwise to the vial. Finally, the reaction vessel was sealed and placed in the dark for 2 days to produce red emission Au clusters. The as-synthesized product Au clusters were dialyzed (Millipore, MWCO: 3 kDa) to cut off free peptides and free ions. The purified sample was stored at 4 °C in the dark for later studies.

Characterizations of the Peptide-Au Cluster. A spectro-fluometer (RF-5301, Shimadzu, Japan) was used to obtain the fluorescence spectra of the peptide−Au cluster (0.5 mM, 200 μL). The mass spectra of the Au cluster were obtained by the ABI MALDI-TOF system in a linear positive mode with a matrix of CHCA.

Cell Toxicity and Apoptosis of CNE1, MCF-7, and 16HBE Cells. The colorimetric cck-8 assay was used to determine the toxicity of free peptide, $Au_5Peptide_3$, and $Au_{22}Peptide_{10}$. CNE1, MCF-7, and 16HBE cells (2×10^3 cells/well) were seeded in 96-well plates individually. After the cells were incubated overnight, $Au_5peptide_3$ and $Au_{22}peptide_{10}$ with various concentrations of Au (4, 10, 20, 40, and 80 μM) and peptide (2, 5, 10, 20, 40, 50, and 100 μM) were added and incubated for 24 h (total volume 200 μL). The used peptide concentrations were kept equal to the peptide concentrations of the peptide−Au cluster. After 24, 36, or 48 h, the medium was removed, 10 μL of cck-8 solution in 100 μL of RPMI Medium Modified was added, and the plate was incubated for 1 h. Then, the absorbance at 450 nm was read using a microplate reader (SpectraMAX M2, Sunnyvale, California). Absorbance values were normalized to control wells and plotted as the concentration of Au versus % cell viability.

For Annexin V-FITC/PI Staining, CNE1 cells (1×10^5) were seeded in a 12-well plate overnight and treated with $Au_5Peptide_3$ and $Au_{22}Peptide_{10}$ (Au concentrations were 0, 20, 40, and 80 μM) for 24 h. Then, the cells were harvested by trypsinization, washed with PBS twice, and resuspended in binding buffer. Annexin V-FITC (5 μL) and propidium iodide (5 μL) were added to the cell suspension (500 μL) for 15 min in the dark at room temperature. The cells were analyzed by flow cytometry (Accuri C6 flow cytometer). Results were analyzed by Cflow software.

Cellular Localization of $Au_5Peptide_3$ and $Au_{22}Peptide_{10}$ in CNE1 Cells. For confocal microscopy study, 1×10^5 CNE1 cells were seeded on a glass bottomed culture dish and incubated for 24 h. Then, $Au_5Peptide_3$ or $Au_{22}Peptide_{10}$ (Au concentration of 80 μM) was added and incubated for 24 h. Cells were then washed with PBS three times and incubated with mitotracker (20 nM) or lysotracker (20 nM) for 20 min. After being washed with PBS three times, the samples were observed by confocal microscopy.

For the SIM microscopy study, 1×10^5 CNE1 cells were seeded on a glass bottomed culture dish and incubated for 24 h. $Au_5Peptide_3$ (80 μM Au) was added and incubated with CNE1 cells for 24 h. Then the cells were washed with PBS and incubated with mitotracker (20 nM) for 20 min. After being washed with PBS three times, the samples were observed by structured-illumination microscopy. Fifteen pictures with moore's stripes were captured by choosing 3D-SIM and then reconstructed with Nikon software.

ICP-MS Study. CNE1 cells (1×10^6) were seeded in a 6-well plate and incubated overnight. $Au_5Peptide_3$ and $Au_{22}Peptide_{10}$ with various concentrations of Au (20, 40, and 80 μM) were added and subsequently incubated for 24 h. Cells were then washed with PBS three times and harvested by trypsinization. Solutions containing cells were centrifuged at 1200 rpm for 3 min and counted with flow cytometry. Subsequently, the cells were divided into two equal parts. One part was used to extract mitochondria by a mitochondrial extraction kit (Beyotime). Then, the two parts were both transferred to MARS Vessels. Nitric acid (67%, 3 mL) and 1 mL of hydrogen peroxide were added to these samples individually overnight. They were digested against the Microwave Reactions System (CEM Co. MARS Xpress). After that, 1 mL of nitric acid (67%) and 3 mL of hydrochloric acid (37%) were added to them overnight and digested again. Finally, an aqueous solution containing 2% HNO_3 and 1% HCl was added to these samples (total volume 3 mL). A series of Au standard solutions (0.5, 1, 5, 10, and 50 ng/mL in an aqueous solution containing 2% HNO_3 and 1% HCl) were injected to obtain the Au standard calibration curve. All of the experiments were performed in triplicates.

Cellular Localization of $Au_5Peptide_3$ by Transmission Electron Microscopy. CNE1 cells (2×10^5 cells/mL) were grown in RPMI modified medium containing 10% fetal bovine serum in a cell incubator for 24 h. Then, two samples were prepared. One was CNE1 cells incubated with $Au_5Peptide_3$ (80 μM Au) for 24 h. The other was control CNE1 cells. After that, the samples were washed with PBS, trypsinized, and centrifuged. Cell beads were collected and fixed with 2.5% glutaraldehyde for 2 h at 4 °C. Then, the samples were washed

DOI: 10.1021/acsnano.8b00027
ACS Nano 2018, 12, 4378−4386

with phosphate buffer and postfixed with 1% osmium tetroxide solution for 2 h at 4 °C. After that, the samples were washed with phosphate buffer, stained with 2% uranium acetate solution for 2 h, and dehydrated in a graded series of acetone (50, 70, 90, and 100%) for 15 min each time at 4 °C. Then, they were impregnated with a 100% acetone:Epon812 embedding medium (1:1 then 1:2) for 1.5 h at room temperature and an Epon812 embedding medium for 3 h at 37 °C. Finally, the samples were sliced into ultrathin sections (the thickness was about 50−80 nm), stained with both uranyl acetate and lead citrate, and imaged with FEI Tecnai G2 TEM.

Western Blot Analysis of CNE1 Cells Treated with $Au_5Peptide_3$. CNE1 cells were seeded in a 6-well plate overnight and treated with $Au_5Peptide_3$ (Au concentrations were 0, 20, 40, and 80 μM) for 24 h. Cell lysates were prepared in a RIPA buffer (Beyotime) and a protease inhibitor cocktail tablet (Roche Molecular Biochemicals) for 10 min at 4 °C. The cell supernatant was collected by being centrifuged at 12000 rpm for 5 min at 4 °C. Protein concentrations of the samples were measured by the BCA assay kit (Beyotime). Then the samples were mixed with 5× loading buffer and heated at 100 °C for 5 min. Proteins with equal amounts were run on 12 or 15% SDS-polyacrylamide gel and then transferred to PVDF membranes. Membranes were blocked with 5% (w/v) nonfat milk in TBST (TBS/0.1% Tween 20) and incubated with the cytochrome c, caspase-9, caspase-3, PARP, bcl-2, bcl-xl, Mcl-1, Bid, Bim, Puma, and β-actin primary antibodies. After being incubated with horseradish peroxidase conjugated second antibodies, protein bands were detected with the Amersham ECLTM Prime Western Blotting Detection Reagent (GE Healthcare, U.K.).

Mitochondrial Membrane Potential Study of CNE1 Cells Treated with $Au_5Peptide_3$. CNE1 (1×10^5) cells were seeded onto a glass bottomed culture dish and incubated for 24 h. $Au_5Peptide_3$ (80 μM Au) was added and incubated for 24 h. After the cells were washed with PBS three times, JC-1 (1.0 μg/mL) in RPMI Medium Modified was treated for 20 min at 37 °C. Then, the stained cells were washed and observed by a confocal microscope.

$Au_5Peptide_3$ Suppresses CNE1 Tumor Growth in the Xenograft Model. All animal care and experiments were conducted in compliance with the requirements of the National Act on the use of experimental animals (China) and were approved by the Institutional Animal Care and Ethic Committee (Approved No. SYXK2016-0048). The severe combined immune deficiency female mice that were four-weeks old (about 15 g per mouse) were divided into four groups, with four mice in each group. We implanted CNE1 cells (10^7 cells per mouse) into the rear flank of each mouse. After that, the four groups of mice were intraperitoneally injected with $Au_5Peptide_3$ (the Au dose was 10 and 15 mg/kg, the volume was 0.2 mL per mouse), physiological saline (0.2 mL per mouse), and a peptide−water solution (110 mg/kg, 0.2 mL per mouse) once every 2 days. We measured the body weights, as well as the tumor volume, by a Vernier caliper every 3 days. Then we calculated the tumor volume by $a \times b^2/2$ (a and b represent the longest and shortest diameter, respectively). After 21 days of $Au_5Peptide_3$ treatments, we sacrificed the mice, as the tumor volumes were obviously very big, and we could not carry the study further.

Immunohistochemistry Study of Tumor Tissue. Paraffin-embedded 4 μm-thick tumor tissues were analyzed by immunehistochemistry using primary antibodies against Mcl-1 and Puma. The tissues were deparaffinized in xylene, rehydrated with a graded series of ethanol, and rinsed in PBS. Then, 3% H_2O_2 was used to inactivate the endogenous peroxide. After that, the tissues were heated for 20 min in sodium citrate buffer at 95 °C and then cooled at room temperature for 20 min. The tissues were then incubated with primary antibodies of Mcl-1 and Puma, followed by being rinsed with 0.2 M PBS. The HRP-conjugated secondary antibody was added for 30 min at 37 °C. After being washed with PBS, DAB solution was applied, incubated at room temperature for 3 min, and counterstained with hematoxylin.

Histology Studies of Tissue. For histology analysis, mice were sacrificed after 21 days of intraperitoneal administration of $Au_5Peptide_3$ (the Au dose was 10 and 15 mg/kg), saline, and a peptide−water solution (110 mg/kg) once every other day. The tissues and organs, including the heart, liver, spleen, lung, and kidney, were collected from these four groups, fixed in 10% formalin, embedded in paraffin, sectioned, and then stained with H&E. The histological slides were observed using an optical microscope.

Au Distributions in Organs and Blood of Nude Mice. For *in vivo* biodistribution assays, mice were sacrificed after 21 days of intraperitoneal administration of $Au_5Peptide_3$ (the Au dose was 10 and 15 mg/kg), physiological saline, and a peptide−water solution (110 mg/kg) once every other day. Blood (50 μL) of each mouse from all of the groups (three mice were in each group) was collected for Au content analysis by ICP-MS. Subsequently, the tumor, heart, liver, spleen, lung, and kidney were collected from these groups. The Au content was quantified by using ICP-MS.

Hematology and Blood Biochemical Assay. After 3 weeks of administration of $Au_5Peptide_3$ (the Au dose was 10 and 15 mg/kg), physiological saline, and a peptide−water solution, blood of the above four groups was collected to carry out the hematological and blood biochemical assay, see Figures S8 and S9.

ASSOCIATED CONTENT

Supporting Information

The Supporting Information is available free of charge on the ACS Publications website at DOI: 10.1021/acsnano.8b00027.

MALDI-TOF-MS spectra, cell viability study of MCF-7 and 16HBE cells, excitation and emission spectra, cck-8 results, flow cytometry results, blood biochemical results, and hematology analysis (PDF)

AUTHOR INFORMATION

Corresponding Author

*E-mail: gaoxy@ihep.ac.cn.

ORCID

Yuliang Zhao: 0000-0002-9586-9360

Xueyun Gao: 0000-0002-2267-9945

Notes

The authors declare no competing financial interest.

ACKNOWLEDGMENTS

This work is supported by grants from the National Natural Science Foundation of China (21425522, 21390414, and 21727817 to X.G.), Beijing Science and Technology Commission Special Project for Frontier Technology in Life Sciences (Z171100000417008 to X.G.), and Beijing municipal high level innovative team building program (IDHT20180504).

REFERENCES

(1) Qian, H.; Zhu, M.; Wu, Z.; Jin, R. Quantum Sized Gold Nanoclusters with Atomic Precision. *Acc. Chem. Res.* **2012**, *45*, 1470−1479.

(2) Mahmoudi, M.; Lynch, I.; Ejtehadi, M. R.; Monopoli, M. P.; Bombelli, F. B.; Laurent, S. Protein-Nanoparticle Interactions: Opportunities and Challenges. *Chem. Rev.* **2011**, *111*, 5610−5637.

(3) He, X.; Zhang, Z.; Liu, J.; Ma, Y.; Zhang, P.; Li, Y.; Wu, Z.; Zhao, Y.; Chai, Z. Quantifying the Biodistribution of Nanoparticles. *Nat. Nanotechnol.* **2011**, *6*, 755.

(4) Jin, R. Atomically Precise Metal Nanoclusters: Stable Sizes and Optical Properties. *Nanoscale* **2015**, *7*, 1549−1565.

(5) Cui, Y.; Wang, Y.; Liu, R.; Sun, Z.; Wei, Y.; Zhao, Y.; Gao, X. Serial Silver Clusters Biomineralized by One Peptide. *ACS Nano* **2011**, *5*, 8684−8689.

(6) Crespo, P.; Litran, R.; Rojas, T. C.; Multigner, M.; de la Fuente, J. M.; Sanchez-Lopez, J. C.; Garcia, M. A.; Hernando, A.; Penades, S.; Fernandez, A. Permanent Magnetism, Magnetic Anisotropy, and Hysteresis of Thiol-Capped Gold Nanoparticles. *Phys. Rev. Lett.* **2004**, *93*, 087204.

DOI: 10.1021/acsnano.8b00027
ACS Nano 2018, 12, 4378−4386

(7) Negishi, Y.; Takasugi, Y.; Sato, S.; Yao, H.; Kimura, K.; Tsukuda, T. Magic-Numbered Au(n) Clusters Protected by Glutathione Monolayers (n = 18, 21, 25, 28, 32, 39): Isolation and Spectroscopic Characterization. *J. Am. Chem. Soc.* **2004**, *126*, 6518−6519.
(8) Chen, S.; Ingram, R. S.; Hostetler, M. J.; Pietron, J. J.; Murray, R. W.; Schaaff, T. G.; Khoury, J. T.; Alvarez, M. M.; Whetten, R. L. Gold Nanoelectrodes of Varied Size: Transition to Molecule-like Charging. *Science* **1998**, *280*, 2098−2101.
(9) Li, G.; Jin, R. Atomically Precise Gold Nanoclusters as New Model Catalysts. *Acc. Chem. Res.* **2013**, *46*, 1749−1758.
(10) Tao, Y.; Li, M.; Ren, J.; Qu, X. Metal Nanoclusters: Novel Probes for Diagnostic and Therapeutic Applications. *Chem. Soc. Rev.* **2015**, *44*, 8636−8663.
(11) Goswami, N.; Luo, Z.; Yuan, X.; Leong, D. T.; Xie, J. Engineering Gold-Based Radiosensitizers for Cancer Radiotherapy. *Mater. Horiz.* **2017**, *4*, 817−831.
(12) Du, B.; Jiang, X.; Das, A.; Zhou, Q.; Yu, M.; Jin, R.; Zheng, J. Glomerular Barrier Behaves as an Atomically Precise Bandpass Filter in a Sub-Nanometre Regime. *Nat. Nanotechnol.* **2017**, *12*, 1096−1102.
(13) Wang, Y.; Cui, Y.; Zhao, Y.; Liu, R.; Sun, Z.; Li, W.; Gao, X. Bifunctional Peptides that Precisely Biomineralize Au Clusters and Specifically Stain Cell Nuclei. *Chem. Commun.* **2012**, *48*, 871−873.
(14) Li, Z.; Zhao, R.; Wu, X.; Sun, Y.; Yao, M.; Li, J.; Xu, Y.; Gu, J. Identification and Characterization of a Novel Peptide Ligand of Epidermal Growth Factor Receptor for Targeted Delivery of Therapeutics. *FASEB J.* **2005**, *19*, 1978−1985.
(15) Yao, Q.; Feng, Y.; Fung, V.; Yu, Y.; Jiang, D.-e.; Yang, J.; Xie, J. Precise Control of Alloying Sites of Bimetallic Nanoclusters *via* Surface Motif Exchange Reaction. *Nat.Commun.* **2017**, *8*, 1555.
(16) Yao, Q.; Yuan, X.; Fung, V.; Yu, Y.; Leong, D. T.; Jiang, D.-e.; Xie, J. Understanding Seed-Mediated Growth of Gold Nanoclusters at Molecular Level. *Nat. Commun.* **2017**, *8*, 927.
(17) Xie, J.; Zheng, Y.; Ying, J. Y. Protein-Directed Synthesis of Highly Fluorescent Gold Nanoclusters. *J. Am. Chem. Soc.* **2009**, *131*, 888−889.
(18) Negishi, Y.; Nobusada, K.; Tsukuda, T. Glutathione-Protected Gold Clusters Revisited: Bridging the Gap between Gold(I)-Thiolate Complexes and Thiolate-Protected Gold Nanocrystals. *J. Am. Chem. Soc.* **2005**, *127*, 5261−5270.
(19) Chua, D. T.; Wei, W. I.; Wong, M. P.; Sham, J. S.; Nicholls, J.; Au, G. K. Phase II Study of Gefitinib for the Treatment of Recurrent and Metastatic Nasopharyngeal Carcinoma. *Head & neck* **2008**, *30*, 863−867.
(20) Weihua, Z.; Tsan, R.; Huang, W. C.; Wu, Q.; Chiu, C. H.; Fidler, I. J.; Hung, M. C. Survival of Cancer Cells is Maintained by EGFR Independent of Its Kinase Activity. *Cancer Cell* **2008**, *13*, 385−393.
(21) Czabotar, P. E.; Lessene, G.; Strasser, A.; Adams, J. M. Control of Apoptosis by the BCL-2 Protein Family: Implications for Physiology and Therapy. *Nat. Rev. Mol. Cell Biol.* **2014**, *15*, 49−63.
(22) Delbridge, A. R.; Grabow, S.; Strasser, A.; Vaux, D. L. Thirty Years of BCL-2: Translating Cell Death Discoveries into Novel Cancer Therapies. *Nat. Rev. Cancer* **2016**, *16*, 99−109.
(23) Adams, J. M.; Cory, S. Bcl-2-Regulated Apoptosis: Mechanism and Therapeutic Potential. *Curr. Opin. Immunol.* **2007**, *19*, 488−496.
(24) Yu, J.; Wang, Z.; Kinzler, K. W.; Vogelstein, B.; Zhang, L. PUMA Mediates the Apoptotic Response to p53 in Colorectal Cancer Cells. *Proc. Natl. Acad. Sci. U. S. A.* **2003**, *100*, 1931−1936.
(25) Jeffers, J. R.; Parganas, E.; Lee, Y.; Yang, C.; Wang, J.; Brennan, J.; MacLean, K. H.; Han, J.; Chittenden, T.; Ihle, J. N.; McKinnon, P. J.; Cleveland, J. L.; Zambetti, G. P. Puma is an Essential Mediator of p53-Dependent and -Independent Apoptotic Pathways. *Cancer Cell* **2003**, *4*, 321−328.
(26) Akgul, C. Mcl-1 is a Potential Therapeutic Target in Multiple Types of Cancer. *Cell. Mol. Life Sci.* **2009**, *66*, 1326−1336.
(27) Andersson, Y.; Juell, S.; Fodstad, O. Downregulation of the Antiapoptotic MCL-1 Protein and Apoptosis in MA-11 Breast Cancer Cells Induced by an Anti-Epidermal Growth Factor Receptor-Pseudomonas Exotoxin a Immunotoxin. *Int. J. Cancer* **2004**, *112*, 475−483.
(28) Liu, B.; Jian, Z.; Li, Q.; Li, K.; Wang, Z.; Liu, L.; Tang, L.; Yi, X.; Wang, H.; Li, C.; Gao, T. Baicalein Protects Human Melanocytes from H(2)O(2)-Induced Apoptosis *via* Inhibiting Mitochondria-Dependent Caspase Activation and the p38 MAPK Pathway. *Free Radical Biol. Med.* **2012**, *53*, 183−193.
(29) Danial, N. N. BCL-2 Family Proteins:Critical Checkpoints of Apoptotic Cell Death. *Clin. Cancer Res.* **2007**, *13*, 7254−7263.

DOI: 10.1021/acsnano.8b00027
ACS Nano 2018, 12, 4378−4386